

Classical double-well systems coupled to finite baths

Hideo Hasegawa*

Department of Physics, Tokyo Gakugei University, Koganei, Tokyo 184-8501, Japan

(Dated: January 31, 2022)

Abstract

We have studied properties of a classical N_S -body double-well system coupled to an N_B -body bath, performing simulations of $2(N_S + N_B)$ first-order differential equations with $N_S \simeq 1 - 10$ and $N_B \simeq 1 - 1000$. A motion of Brownian particles in the absence of external forces becomes chaotic for appropriate model parameters such as N_B , c_o (coupling strength), and $\{\omega_n\}$ (oscillator frequency of bath): For example, it is chaotic for a small N_B ($\lesssim 100$) but regular for a large N_B ($\gtrsim 500$). Detailed calculations of the stationary energy distribution of the system $f_S(u)$ (u : an energy per particle in the system) have shown that its properties are mainly determined by N_S , c_o and T (temperature) but weakly depend on N_B and $\{\omega_n\}$. The calculated $f_S(u)$ is analyzed with the use of the Γ distribution. Difference and similarity between properties of double-well and harmonic-oscillator systems coupled to finite bath are discussed.

PACS numbers: 05.40.-a, 05.70.-a, 05.10.Gg

*hideohasegawa@goo.jp

I. INTRODUCTION

Many studies have been made with the use of a model describing a classical or quantum open system which is coupled to baths consisting of a collection of harmonic oscillators. Such a model is conventionally referred to as the Caldeira-Leggett (CL) model [1, 2], although equivalent models had been proposed earlier by Magalinskii [3] and Ullersma [4]. From the CL model, we may derive the Langevin model with dissipation and diffusion (noise) terms. Originally the CL model was introduced for N_B -body bath with $N_B \rightarrow \infty$, for which the Ohmic and Drude-type spectral densities with continuous distributions are adopted. Furthermore in the original CL model, the number of particles in a systems, N_S , is taken to be unity ($N_S = 1$). We expect that a generic open system may contain any number of particles and that a system may be coupled to a bath consisting of finite harmonic oscillators in general. In recent years, the CL model has been employed for a study of properties of open systems with finite N_S and/or N_B [5–13]. Specific heat anomalies of quantum oscillator (system) coupled to finite bath have been studied [5, 6, 12]. A thermalization [7, 8], energy exchange [9], dissipation [11] and the Jarzynski equality [13, 14] in classical systems coupled to finite bath have been investigated.

In a previous paper [10], we have studied the $(N_S + N_B)$ model for finite N_S -body systems coupled to baths consisting of N_B harmonic oscillators. Our study for open harmonic oscillator systems with $N_S \simeq 1 - 10$ and $N_B \simeq 10 - 1000$ has shown that stationary energy distribution of the system has a significant and peculiar dependence on N_S , but it weakly depends on N_B [10]. These studies mentioned above [5–13] have been made for harmonic-oscillator systems with finite N_S and/or N_B .

Double-well potential models have been employed in a wide range of fields including physics, chemistry and biology (for a recent review on double-well system, see Ref. [15]). Various phenomena such as the stochastic resonance (SR), tunneling through potential barrier and thermodynamical properties [16] have been studied. The CL model for the double-well systems with $N_S = 1$ and $N_B = \infty$ has been extensively employed for a study on the SR [17]. Properties of SR for variations of magnitude of white noise [17–20] and relaxation time of colored noise [21, 22] have been studied. However, studies for open double-well systems with finite N_S and/or N_B have not been reported as far as we are aware of. It would be interesting and worthwhile to study open classical double-well systems described by the

$(N_S + N_B)$ model with finite N_S and N_B , which is the purpose of the present paper.

The paper is organized as follows. In Sec. II, we briefly explain the $(N_S + N_B)$ model proposed in our previous study [10]. In Sec. III, direct simulations (DSs) of $2(N_S + N_B)$ first-order differential equations for the adopted model have been performed. Dynamics of a single double-well system ($N_S = 1$) coupled to a finite bath ($2 \leq N_B \leq 1000$) in the phase space is investigated (Sec. III B). We study stationary energy distributions in the system and bath, performing detailed DS calculations, changing N_S , N_B , the coupling strength and the distribution of bath oscillators (Sec. III C). Stationary energy and position distributions obtained by DSs are analyzed in Sec. IV. The final Sec. V is devoted to our conclusion.

II. ADOPTED $(N_S + N_B)$ MODEL

We consider a system including N_S Brownian particles coupled to a bath consisting of independent N_B harmonic oscillators. We assume that the total Hamiltonian is given by [10]

$$H = H_S + H_B + H_I, \quad (1)$$

with

$$H_S = \sum_{k=1}^{N_S} \left[\frac{P_k^2}{2M} + V(Q_k) \right], \quad (2)$$

$$H_B = \sum_{n=1}^{N_B} \left[\frac{p_n^2}{2m} + \frac{m\omega_n^2}{2} q_n^2 \right], \quad (3)$$

$$H_I = \frac{1}{2} \sum_{k=1}^{N_S} \sum_{n=1}^{N_B} c_{kn} (Q_k - q_n)^2, \quad (4)$$

where H_S , H_B and H_I express Hamiltonians for the system, bath and interaction, respectively. Here M (m) denotes the mass, P_k (p_n) the momentum, Q_k (q_n) position of the oscillator in the system (bath), $V(Q_k)$ signifies the potential in the system, ω_n stands for oscillator frequency in the bath, and c_{nk} is coupling constant. The model is symmetric with respect to an exchange of system \leftrightarrow bath if $V(Q)$ is the harmonic potential. From Eqs.

(1)-(4), we obtain $2(N_S + N_B)$ first-order differential equations,

$$\dot{Q}_k = \frac{P_k}{M}, \quad (5)$$

$$\dot{P}_k = -V'(Q_k) - \sum_{n=1}^{N_B} c_{kn}(Q_k - q_n), \quad (6)$$

$$\dot{q}_n = \frac{p_n}{m}, \quad (7)$$

$$\dot{p}_n = -m\omega_n^2 q_n - \sum_{k=1}^{N_S} c_{kn}(q_n - Q_k), \quad (8)$$

which yield

$$M\ddot{Q}_k = -V'(Q_k) - \sum_{n=1}^{N_B} c_{kn}(Q_k - q_n), \quad (9)$$

$$m\ddot{q}_n = -m\omega_n^2 q_n - \sum_{k=1}^{N_S} c_{kn}(q_n - Q_k), \quad (10)$$

with prime ($'$) and dot ($\dot{\cdot}$) denoting derivatives with respect to the argument and time, respectively. It is noted that the second term of Eq. (6) or (9) given by

$$F_k^{(eff)} = - \sum_{n=1}^{N_B} c_{kn}(Q_k - q_n), \quad (11)$$

plays a role of the effective force to the k th system.

A formal solution of Eq. (10) for $q_n(t)$ is given by

$$q_n(t) = q_n(0) \cos \tilde{\omega}_n t + \frac{\dot{q}_n(0)}{\tilde{\omega}_n} \sin \tilde{\omega}_n t + \sum_{\ell=1}^{N_S} \frac{c_{\ell n}}{m\tilde{\omega}_n} \int_0^t \sin \tilde{\omega}_n(t-t') Q_\ell(t') dt', \quad (12)$$

with

$$\tilde{\omega}_n^2 = \frac{b_n}{m} + \sum_{k=1}^{N_S} \frac{c_{kn}}{m} = \omega_n^2 + \sum_{k=1}^{N_S} \frac{c_{kn}}{m}. \quad (13)$$

Substituting Eq. (12) to Eq. (9), we obtain the non-Markovian Langevin equation given by

$$\begin{aligned} M\ddot{Q}_k(t) = & -V'(Q_k) - M \sum_{\ell=1}^{N_S} \xi_{k\ell} Q_\ell(t) - \sum_{\ell=1}^{N_S} \int_0^t \gamma_{k\ell}(t-t') \dot{Q}_\ell(t') dt' \\ & - \sum_{\ell=1}^{N_S} \gamma_{k\ell}(t) Q_\ell(0) + \zeta_k(t) \quad (k = 1 \text{ to } N_S), \end{aligned} \quad (14)$$

with

$$M\xi_{k\ell} = \sum_{n=1}^{N_B} \left[c_{kn}\delta_{k\ell} - \frac{c_{kn}c_{\ell n}}{m\tilde{\omega}_n^2} \right], \quad (15)$$

$$\gamma_{k\ell}(t) = \sum_{n=1}^{N_B} \left(\frac{c_{kn}c_{\ell n}}{m\tilde{\omega}_n^2} \right) \cos \tilde{\omega}_n t, \quad (16)$$

$$\zeta_k(t) = \sum_{n=1}^{N_B} c_{kn} \left[q_n(0) \cos \tilde{\omega}_n t + \frac{\dot{q}_n(0)}{\tilde{\omega}_n} \sin \tilde{\omega}_n t \right], \quad (17)$$

where $\xi_{k\ell}$ denotes the additional interaction between k and ℓ th particles in the system induced by couplings $\{c_{kn}\}$, $\gamma_{k\ell}(t)$ the memory kernel and ζ_k the stochastic force.

If the equipartition relation is realized in initial values of $q_n(0)$ and $\dot{q}(0)$,

$$\langle m\tilde{\omega}_n^2 q_n(0)^2 \rangle_B = \langle m\dot{q}_n(0)^2 \rangle_B = k_B T, \quad (18)$$

we obtain the fluctuation-dissipation relation:

$$\langle \zeta_k(t)\zeta_k(t') \rangle_B = k_B T \gamma_{kk}(t - t'), \quad (19)$$

where $\langle \cdot \rangle_B$ stands for the average over variables in the bath.

In the case of $N_B \rightarrow \infty$, summations in Eqs. (15)-(17) are replaced by integrals. When the spectral density defined by

$$J(\omega) = \frac{\pi}{2} \sum_n \frac{c_n^2}{m_n \omega_n^2} \delta(\omega - \omega_n), \quad (20)$$

is given by the Ohmic form: $J(\omega) \propto \omega$ for $0 \leq \omega < w_D$, the kernel becomes

$$\gamma(t) \propto \frac{\sin \omega_D t}{\pi t} \propto \delta(t), \quad (21)$$

which leads to the Markovian Langevin equation.

In the case of $N_S = 1$, we obtain ξ and γ in Eqs. (15) and (16) where the subscripts k and ℓ are dropped (*e.g.*, $c_{kn} = c_n$),

$$M\xi(t) = \sum_{n=1}^{N_B} c_n \left(1 - \frac{c_n}{m\tilde{\omega}_n^2} \right), \quad (22)$$

$$\gamma(t) = \sum_{n=1}^{N_B} \left(\frac{c_n^2}{m\tilde{\omega}_n^2} \right) \cos \tilde{\omega}_n t. \quad (23)$$

The additional interaction vanishes ($\xi = 0$) if we choose $c_n = m\tilde{\omega}_n^2$ in Eq. (22).

In the case of $N_S \neq 1$, however, it is impossible to choose $\{c_{kn}\}$ such that $\xi_{k\ell} = 0$ is realized for all pairs of (k, ℓ) in Eq. (15). Then Q_k is inevitably coupled to Q_ℓ for $\ell \neq k$ with the superexchange-type interaction of antiferromagnets: $-\sum_n c_{kn}c_{\ell n}/m\tilde{\omega}_n^2$ in Eq. (15).

III. MODEL CALCULATIONS FOR DOUBLE-WELL SYSTEMS

A. Calculation methods

We consider a system with the double-well potential

$$V(Q) = \left(\frac{\Delta}{Q_0^4} \right) (Q^2 - Q_0^2)^2, \quad (24)$$

which has the stable minima of $V(\pm Q_0) = 0$ at $Q = \pm Q_0$ and locally unstable maximum of $V(0) = \Delta$ at $Q = 0$ with the barrier height Δ . We have adopted $Q_0 = 1.0$ and $\Delta = 1.0$ in our DSs.

It is easier to solve $2(N_S + N_B)$ first-order differential equations given by Eqs. (5)-(8) than to solve the N_S Langevin equations given by Eqs. (14)-(17) although the latter provides us with clearer physical insight than the former. In order to study the N_S and N_B dependences of various physical quantities, we have assumed that the coupling c_{kn} is given by [10, 24]

$$c_{kn} = \frac{c_o}{N_S N_B}, \quad (25)$$

because the interaction term includes summations of $\sum_{k=1}^{N_S}$ and $\sum_{n=1}^{N_B}$ in Eq. (4). It is noted that with our choice of c_{kn} , the interaction contribution is finite even in the thermodynamical limit of $N_B \rightarrow \infty$ because the summation over n runs from 1 to N_B in Eq. (4). DSs of Eqs. (5)-(8) have been performed with the use of the fourth-order Runge-Kutta method with the time step of 0.01. We have adopted $k_B = 1.0$, $M = m = 1.0$, $c_o = 1.0$, and $\omega_n = 1.0$ otherwise noticed.

We consider energies per particle $u_\eta(t)$ in the system ($\eta=S$) and the bath ($\eta=B$) which are assume to be given by

$$u_S = \frac{1}{N_S} \sum_{k=1}^{N_S} \left[\frac{P_k^2}{2M} + V(Q_k) \right], \quad (26)$$

$$u_B = \frac{1}{N_B} \sum_{n=1}^{N_B} \left[\frac{p_n^2}{2m} + \frac{m\omega_n^2 q_n^2}{2} \right], \quad (27)$$

which is valid for the weak interaction, although a treatment of the finite interaction is ambiguous and controversial [5, 6].

B. Dynamics of a particle in the (Q, P) phase space

1. Effect of c_o

First we consider an isolated double-well system ($N_S = 1$ and $c_o = 0.0$). Figure 1 shows the phase-space trajectories in the (Q, P) phase space for this system with six different initial system energies E_{So} . For $E_{So} = 0.0$, the system has two stable fixed points at $(Q, P) = (\pm 1.0, 0.0)$, and for $E_{So} = \Delta = 1.0$ it has one unstable fixed point at $(Q, P) = (0.0, 0.0)$. In the case of $0.0 < E_{So} < 1.0$, the trajectory is restricted in the region of $Q > 0.0$ (or $Q < 0.0$). In contrast in the case of $E_{So} > 1.0$, trajectory may visit both regions of $Q > 0.0$ and $Q < 0.0$. The case of $E_{So} = 1.0$ is critical between the two cases.

Next the double-well system is coupled to a bath. In our DSs, we have assumed that system and bath are decoupled at $t < 0$ where they are in equilibrium states with $E_{So} = T$, the temperature T being defined by $T = u_B$. We have chosen initial values of $Q(0) = 1.0$ and $P(0) = \sqrt{2M[E_{So} - V(Q(0))]}$ for a given initial system energy E_{So} . Initial conditions for $q_n(0)$ and $p_n(0)$ are given by random Gaussian variables with zero means and variance proportional to T [Eq. (18)] [10]. Results to be reported in this subsection have been obtained by single runs for $t = 0$ to 1000.

Figures 2(a) and 2(b) show a strobe plot in the (Q, P) phase space (with a time interval of 1.0) and the time-dependence of $Q(t)$, respectively, for $E_{So} = 1.0$, $N_S = 1$, $N_B = 100$ and $c_o = 0.2$. The trajectory starting from $Q(0) = 1.0$ goes to the negative- Q region because a particle may go over the potential barrier with a help of a force (noise) originating from bath given by Eq. (11). The system energy fluctuates as shown in Fig. 2(c), whose distribution is plotted in Fig. 2(d).

Results in Fig. 2 are regular. In contrast, when a coupling strength is increased to $c_o = 1.0$, the system becomes chaotic as shown in Figs. 3(a) and 3(b) where a strobe plot in the (Q, P) phase space and the time-dependence of $Q(t)$ are plotted, respectively. This is essentially the force-induced chaos in classical double-well system [23]: although an external force is not applied to our system, a force arising from a coupling with bath given by Eq. (11) plays a role of an effective external force for the system. Figures 3(c) and 3(d) show that in the case of $c_o = 1.0$, u_S has more appreciable temporal fluctuations with a wider energy distribution in $f_S(u)$ than in the case of $c_o = 0.2$. Although system energies fluctuate, they

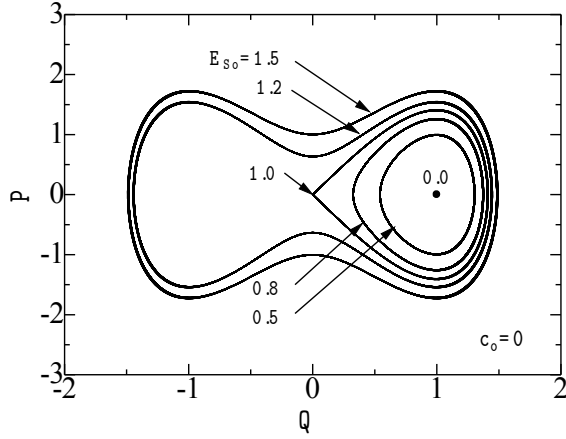


FIG. 1: Plot of phase-space trajectories for a particle in an isolated double-well system ($c_o = 0.0$). Trajectories are plotted for energies of $E_{So}/\Delta = 0.0, 0.5, 0.8, 1.0, 1.2$ and 1.5 .

are not dissipative at $0.0 \leq t < 1000.0$ in DSs both for $c_o = 0.2$ and $c_o = 1.0$ with $N_B = 100$.

2. Effect of ω_n distributions

We have so far assumed $\omega_n = 1.0$ in the bath, which is now changed. Figures 4(a) and 4(c) show strobe plots for $\omega_n = 0.5$ and 2.0 , respectively, which are regular and which are different from a chaotic result for $\omega_n = 1.0$ shown in Fig. 4(b). When we adopt $\{\omega_n\}$ which is randomly distributed in $[0.5, 2.0]$, a motion of a system particle becomes chaotic as shown

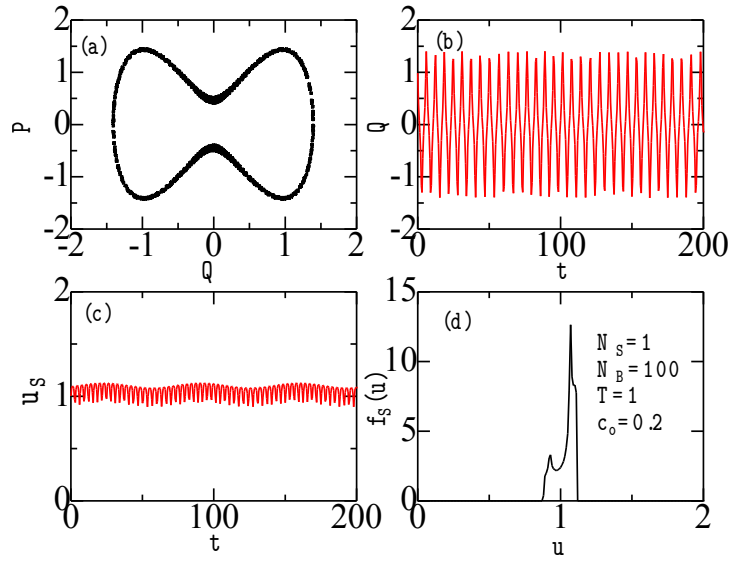


FIG. 2: (Color online) (a) Strobe plot in the (Q, P) phase space (with a time interval of 1.0), (b) $Q(t)$, (c) $u_S(t)$, and (d) the system energy distribution $f_S(u)$ obtained by a single run for $E_{So} = 1.0$, $N_S = 1$, $N_B = 100$, $T = 1.0$ and $c_o = 0.2$.

in Fig. 4(d). This is because contributions from $\omega_n \sim 1.0$ among $[0.5, 2.0]$ induce chaotic behavior.

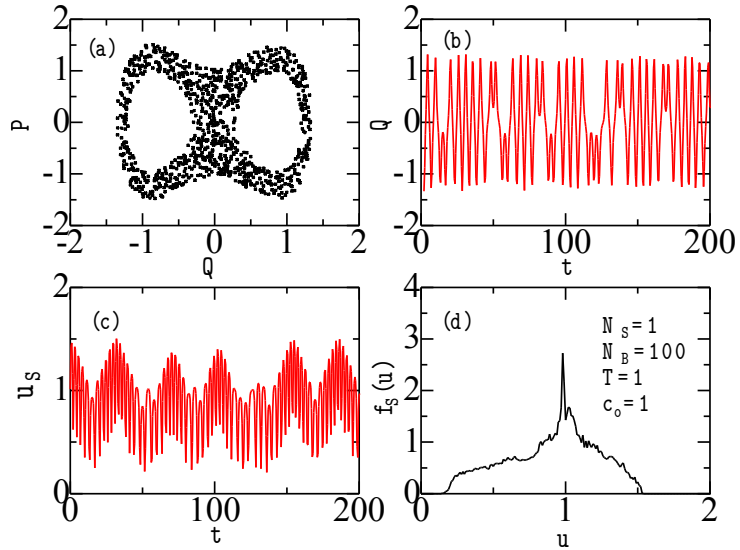


FIG. 3: (Color online) (a) Strobe plot in the (Q, P) phase space, (b) $Q(t)$, (c) $u_S(t)$, and (d) the system energy distribution $f_S(u)$ obtained by a single run for $E_{So} = 1.0$, $N_S = 1$, $N_B = 100$, $T = 1.0$ and $c_o = 1.0$.

3. Effect of N_B

We have repeated calculations by changing N_B , whose results are plotted in Figs. 5(a)-5(d). Figures 5(a), 5(b) and 5(c) show that chaotic behaviors for $N_B = 2$ and $N_B = 10$ are

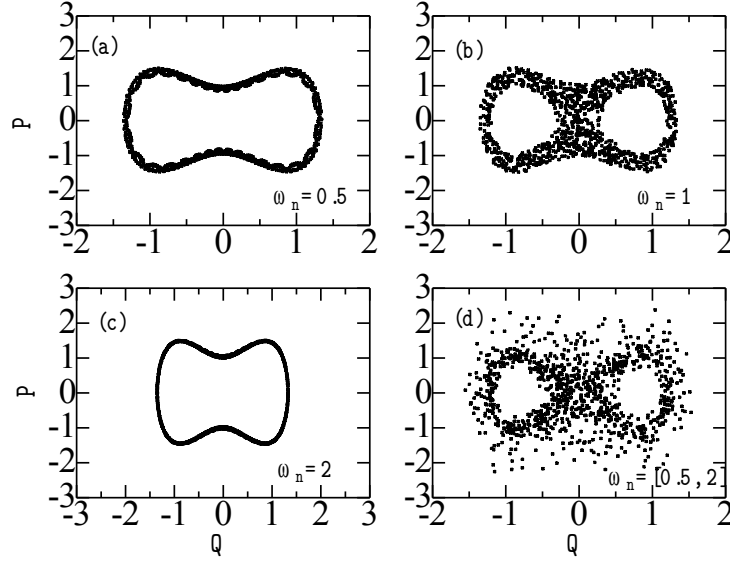


FIG. 4: Strobe plots in the (Q, P) phase space for various distribution of $\{\omega_n\}$: (a) $\omega_n = 0.5$, (b) $\omega_n = 1.0$, (c) $\omega_n = 2.0$ and (d) $\omega_n \in [0.5, 2.0]$ obtained by single runs with $E_{So} = 1.0$, $N_S = 1$, $N_B = 100$, $T = 1.0$ and $c_o = 1.0$.

more significant than that for $N_B = 100$. On the contrary, chaotic behavior is not realized for $N_B = 1000$ in Fig. 5(d), which is consistent with the fact that chaos has not been reported for the double-well system subjected to infinite bath.

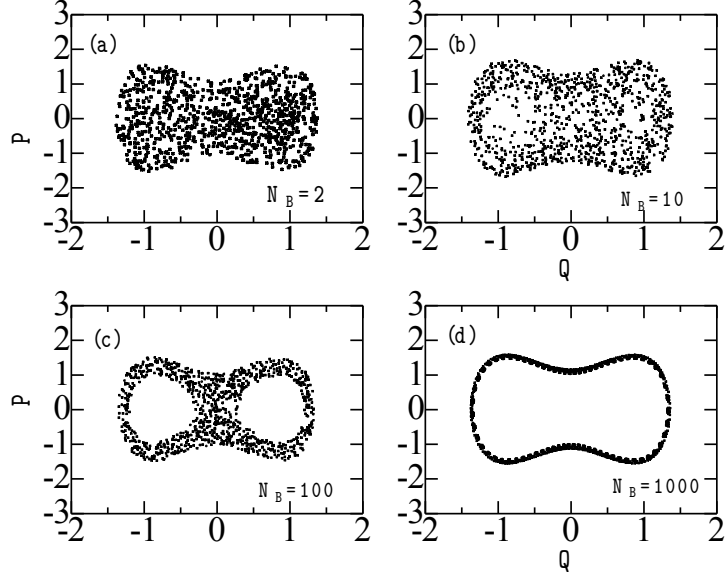


FIG. 5: Strobe plots in the (Q, P) phase space for various N_B : (a) $N_B = 2$, (b) $N_B = 10$, (c) $N_B = 100$ and (d) $N_B = 1000$ with $E_{So} = 1.0$, $N_S = 1$, $T = 1.0$ and $c_o = 1.0$.

4. Effect of initial system energy E_{So}

Next we change the initial system energy of E_{So} . Figures 6(a)-(d) show strobe plots in the (Q, P) phase space for various E_{So} with $N_S = 1$, $N_B = 100$, $T = 1.0$ and $c_o = 1.0$. Figure 6(a) shows that for $E_{So} = 0.5$, the regular trajectory starting from $Q = 1.0$ remains

in the positive- Q region because a particle cannot go over the potential barrier of $\Delta = 1.0$. For $E_{So} = 0.8$, chaotic trajectories may go to the negative- Q region with a help of force from bath [Eq. 11]. Figure 6(d) shows that when E_{So} is too large compared to Δ ($E_{So}/\Delta = 1.2$), the trajectory again becomes regular, going between positive- and negative- Q regions.

Figure 7 shows the system energy distribution $f_S(u)$ for various E_{So} . $f_S(u)$ moves upward as E_{So} is increased. It is noted that peak positions of $f_S(u)$ for $E_{So} = 0.5 - 1.0$ locate at $u \simeq 1.0$ while that for $E_{So} = 1.2$ locates at $u \simeq 1.35$.

C. Stationary energy probability distributions

In this subsection, we will study stationary energy probability distributions of system and bath which are averaged over N_r ($=10\,000$) runs starting from different initial conditions. Assuming that the system and bath are in the equilibrium states with $T = u_B = u_S$ at $t < 0.0$, we first generate exponential derivatives of initial system energies $\{E_j\}$: $p(E_j) \propto \exp(-\beta E_j)$ ($j = 1$ to $N_S N_r$) for our DSs where $\beta = 1/k_B T$. A pair of initial values of $Q_j(0)$ and $P_j(0)$ for a given E_j is randomly chosen such that they meet the condition given by $E_j = P_j(0)^2/2M + V(Q_j(0))$. The procedure for choosing initial values of $q_n(0)$ and $p_n(0)$ is the same as that adopted in the preceding subsection [10]. We have discarded results for $t < 200$ in our DSs performed for $t = 0$ to 1000.

Before discussing cases where N_S and N_B may be greater than unity, we first study a pedagogical simple case of $N_S = N_B = 1$: a particle with double-well potential is subjected to a single harmonic oscillator. Double-chain curves in Fig. 8(a) and 8(b) show energy distributions of the system $[f_S(u)]$ and bath $[f_B(u)]$, respectively, with $c_o = 0.0$, where $u = u_S$ ($u = u_B$) for the system (bath). Both $f_S(u_S)$ and $f_B(u_B)$ follow the exponential distribution because the assumed initial equilibrium states of decoupled system and bath persist at $t \geq 0.0$. When they are coupled by a weak coupling of $c_o = 0.1$ at $t \geq 0.0$, $f_S(u)$ and $f_B(u)$ almost remain exponential distributions except for that $f_S(u)$ has a small peak at $u = 1.0$, as shown by dashed curve in Fig. 8(a). This peak has been realized in Figs. 2(d) and 3(d). It is due to the presence of a potential barrier with $\Delta = 1.0$ in double-well potential because the peak at $u = 1.0$ in $f_S(u)$ is realized even when $T \neq 1.0$, as will be discussed later in 4. *Effect of T* (Fig. 12). This peak is developed for stronger couplings of $c_o = 1.0$ and 2.0, for which magnitudes of $f_S(u)$ at small u are decreased, as shown by solid

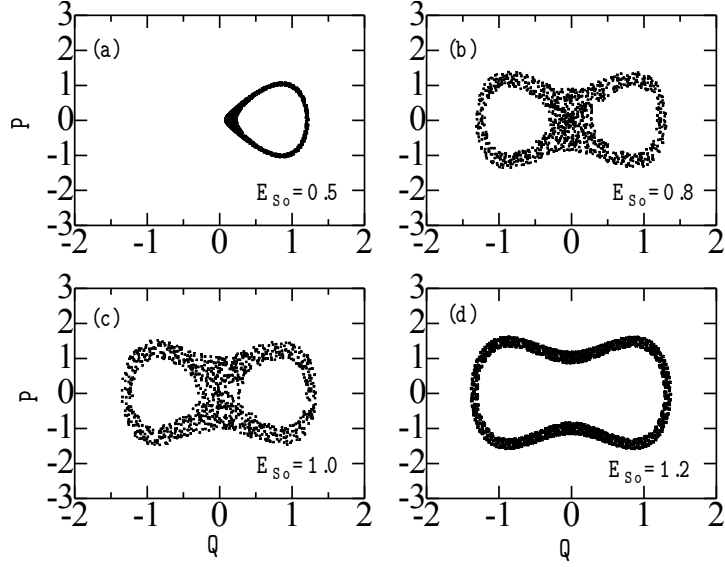


FIG. 6: Strobe plots in the (Q, P) phase space for various E_{So} : (a) $E_{So} = 0.5$, (b) $E_{So} = 0.8$ (c) $E_{So} = 1.0$ and $E_{So} = 1.2$ with $N_S = 1$, $N_B = 100$, $T = 1.0$ and $c_o = 1.0$.

and chain curves in Figs. 8(a) and 8(b).

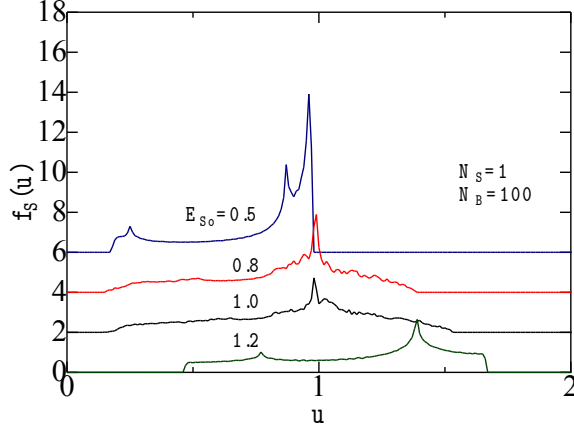


FIG. 7: (Color online) System energy distributions $f_S(u)$ for $E_{S_0} = 0.5, 0.8, 1.0$ and 1.2 with $N_S = 1$, $N_B = 100$, $T = 1.0$ and $c_o = 1.0$, curves being successively shifted upward by two for clarity of figures.

1. Effect of c_o

We change the coupling strength of c_o . Figures 9(a) and 9(b) show $f_S(u)$ and $f_B(u)$, respectively, for $c_o = 0.2, 1.0, 5.0$ and 10.0 with $N_S = 1$, $N_B = 100$ and $T = 1.0$. $f_S(u)$ for $c_o = 0.2$ nearly follows the exponential distribution. When c_o becomes larger, magnitudes of $f_S(u)$ at $u < 1.0$ are decreased while that at $u > 1.0$ is increased. In particular, the magnitude of $f_S(0)$ is more decreased for larger c_o .

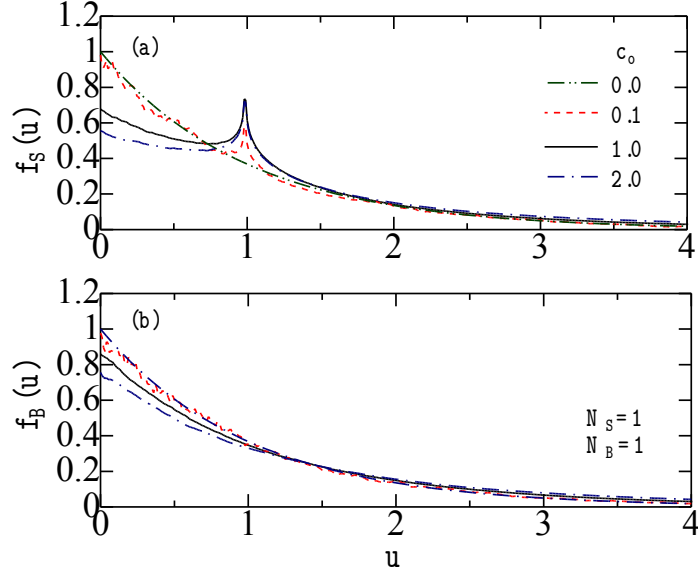


FIG. 8: (Color online) Stationary distributions of (a) $f_S(u)$ and (b) $f_B(u)$ for various c_o : $c_o = 0.0$ (double-chain curves), 0.1 (dashed curves), 1.0 (solid curves) and 2.0 (chain curves) obtained by 10 000 runs with $N_S = N_B = 1$ and $T = 1.0$.

2. Effect of ω_n distributions

Although we have assumed $\omega_n = 1.0$ in both oscillators, we will examine the effect of their distribution, taking into account two kinds of random distributions given by $\omega_n \in [0.5, 2.0]$

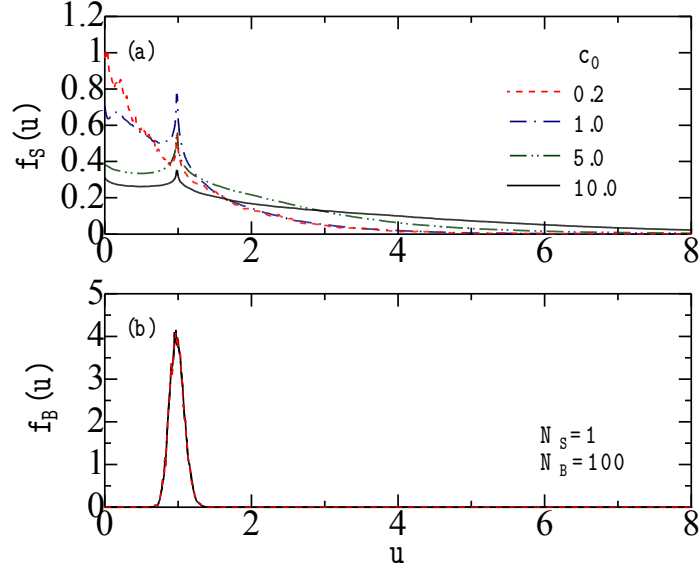


FIG. 9: (Color online) Stationary distributions of (a) $f_S(u)$ and (b) $f_B(u)$ for various c_o : $c_o = 0.2$ (dashed curves), 1.0 (chain curves), 5.0 (double-chain curves) and 10.0 (solid curves) with $N_S = 1$, $N_B = 100$ and $T = 1.0$.

and $\omega_n \in [2.0, 3.0]$. From calculated results shown in Figs. 10(a) and 10(b), we note that $f_S(u)$ and $f_B(u)$ are not much sensitive to the distribution of $\{\omega_n\}$ in accordance with our previous calculation for harmonic oscillator system [10, 25]. This conclusion, however, might

not be applied to the case of infinite bath where distribution of $\{\omega_n\}$ becomes continuous distribution. Ref. [8] reported that the relative position between oscillating frequency ranges of system and bath is very important for a thermalization of the harmonic oscillator system subjected to finite bath.

3. *Effect of N_B*

We have calculated $f_S(u)$ and $f_B(u)$, changing N_B but with fixed $N_S = 1$, whose results are shown in Figs. 11(a) and 11(b). For larger N_B , the width of $f_B(u)$ becomes narrower as expected. However, shapes of $f_S(u)$ are nearly unchanged for all cases of $N_B = 1, 10, 100$ and 1000.

4. *Effect of T*

We change the temperature of the bath. Figures 12(a) and 12(b) show $f_S(u)$ and $f_B(u)$, respectively, for $T = 0.5, 1.0$ and 1.5 with $N_S = 1$, $N_B = 100$ and $c_o = 1.0$. When T is decreased (increased), positions of $f_B(u)$ move to lower (higher) energy such that mean values of u_B correspond to T . For a lower temperature of $T = 0.5$, magnitude of $f_S(u)$ at $u < 1.0$ is increased while that at $u > 1.0$ is decreased. The reverse is realized for higher temperature of $T = 1.5$. We should note that the peak position in $f_S(u)$ at $u = 1.0$ is not changed even if T is changed because this peak is related to the barrier with $\Delta = 1.0$ of the double-well potential.

5. *Effect of N_S*

Although $N_S = 1$ has been adopted so far, we will change N_s to investigate its effects on stationary energy distributions. Figure 13(a) shows $f_S(u)$ for $N_S = 1, 2, 5$ and 10 . $f_S(u)$ for $N_S = 1$ shows an exponential-like distribution with $f_S(0) \neq 0$ at $u = 0.0$. In contrast, $f_S(u)$ vanishes at $u = 0.0$ for $N_S = 2, 5$ and 10 . Figure 13(a) shows that shapes of $f_S(u)$ much depend on N_S while those of $f_B(u)$ are almost unchanged in Fig. 13(b).

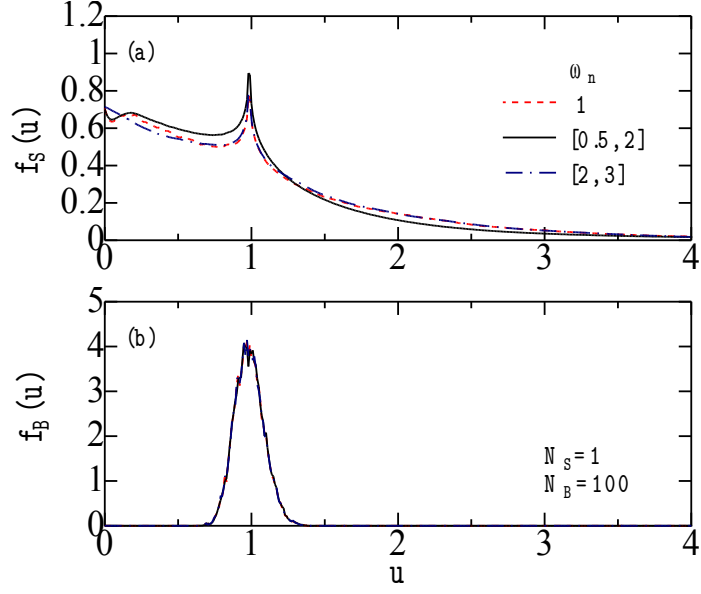


FIG. 10: (Color online) Stationary distributions of (a) $f_S(u)$ and (b) $f_B(u)$ for various distributions of $\{\omega_n\}$: $\omega = 1.0$ (dashed curves), $\omega_n \in [0.5, 2.0]$ (solid curves) and $\omega_n \in [2.0, 3.0]$ (chain curves) with $N_S = 1$, $N_B = 100$, $T = 1.0$ and $c_o = 1.0$.

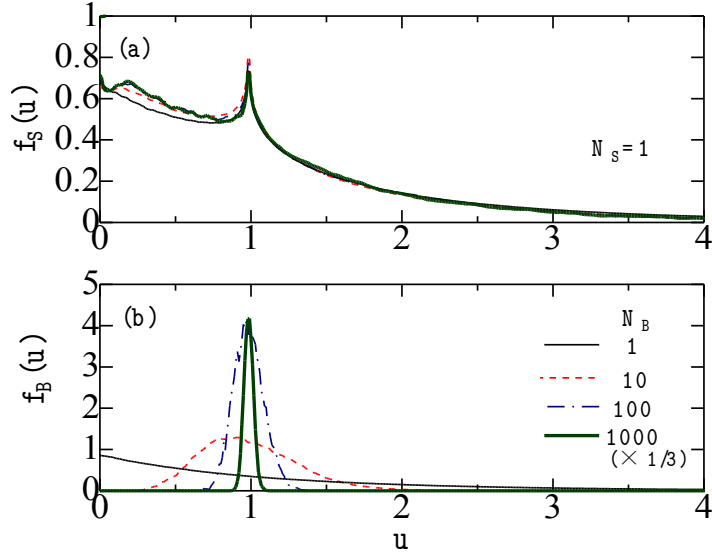


FIG. 11: (Color online) Stationary distributions of (a) $f_S(u)$ and (b) $f_B(u)$ for various N_B : $N_B = 1$ (solid curves), 10 (dashed curves), 100 (chain curves) and 1000 (bold solid curves) with $N_S = 1$, $T = 1.0$ and $c_o = 1.0$. $f_B(u)$ for $N_B = 1000$ is multiplied by a factor of $1/3$.

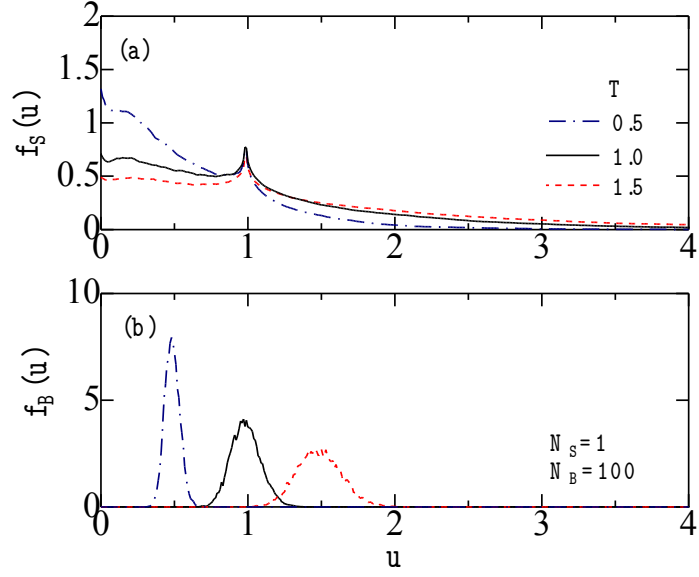


FIG. 12: (Color online) Stationary distributions of (a) $f_S(u)$ and (b) $f_B(u)$ for various T : $T = 0.5$ (chain curves), 1.0 (solid curves) and 1.5 (dashed curves) with $N_S = 1$, $N_B = 100$ and $c_o = 1.0$.

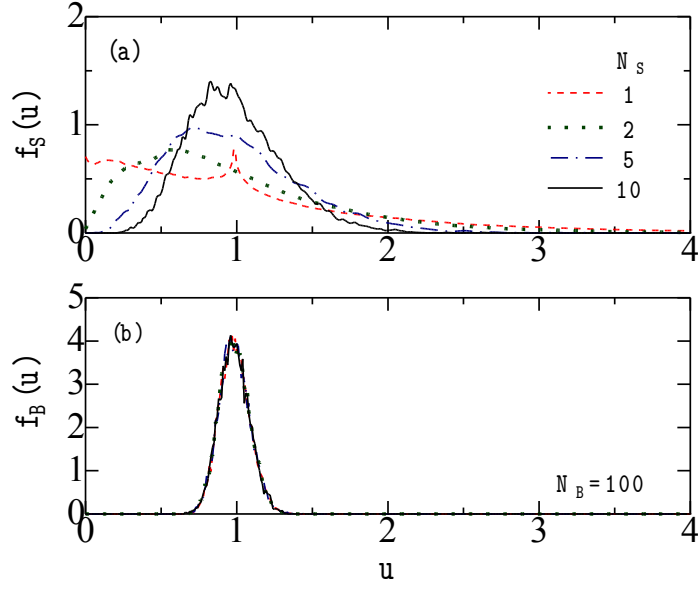


FIG. 13: (Color online) Stationary distributions of (a) $f_S(u)$ and (b) $f_B(u)$ for various N_S : $N_S = 1$ (dashed curves), 2 (dotted curves), 5 (chain curves) and 10 (solid curves) with $N_B = 100$, $T = 1.0$ and $c_o = 1.0$.

IV. DISCUSSION

A. Analysis of stationary energy distributions

Our DSs in the preceding section have shown that $f_S(u)$ depends mainly on N_S , c_o and T while $f_B(u)$ depends mostly on N_B and T for $N_S \ll N_B$. We will try to analyze $f_S(u)$ and $f_B(u)$ in this subsection. It is well known that when variables of x_i ($i = 1 - N$) are independent and follow the exponential distributions with the same mean, the distribution of its sum: $X = \sum_i x_i$ is given by the Γ distribution. Then for an uncoupled system ($c_o = 0.0$), $f_S(u)$ and $f_B(u)$ are expressed by the Γ distribution $g(u)$ given by [10]

$$f_\eta(u) = \frac{1}{Z_\eta} u^{a_\eta-1} e^{-b_\eta u} \equiv g(u; a_\eta, b_\eta), \quad (28)$$

with

$$a_\eta = N_\eta, \quad b_\eta = N_\eta \beta, \quad (29)$$

$$Z_\eta = \frac{\Gamma(a_\eta)}{b_\eta^{a_\eta}}, \quad (30)$$

where $\eta = S$ and B for a system and bath, respectively, and $\Gamma(x)$ is the gamma function. In the limit of $N_S = 1$, the Γ distribution reduces to the exponential distribution. Mean (μ_η) and variance (σ_η^2) of the Γ distribution are given by

$$\mu_\eta = \frac{a_\eta}{b_\eta}, \quad \sigma_\eta^2 = \frac{a_\eta}{b_\eta^2}, \quad (31)$$

from which a_η and b_η are expressed in terms of μ_η and σ_η

$$a_\eta = \frac{\mu_\eta^2}{\sigma_\eta^2}, \quad b_\eta = \frac{\mu_\eta}{\sigma_\eta^2}. \quad (32)$$

We have tried to evaluate $f_S(u)$ and $f_B(u)$ for the coupled system ($c_o \neq 0.0$) as follows: From mean (μ_η) and root-mean-square (RMS) (σ_η) calculated by DSs, a_η and b_η are determined by Eq. (32), with which we obtain the Γ distributions for $f_S(u)$ and $f_B(u)$. Filled and open squares in Fig. 14 show μ_B and σ_B , respectively, as a function of N_S . We obtain $\mu_B = 1.0$ and $\sigma_B = 0.1$ nearly independently of N_S , which yield $a_B = b_B = 100.0$ in agreement with Eq. (29). Filled and open triangles in Fig. 14 express the N_S dependence of μ_S and σ_S obtained by DSs with $c_o = 1.0$, $N_B = 100$ and $T = 1.0$. Calculated mean and RMS values of (μ_S, σ_S) are (1.07, 0.98), (0.99, 0.70), (0.99, 0.44) and (0.99, 0.319) for $N_S = 1, 2, 5$

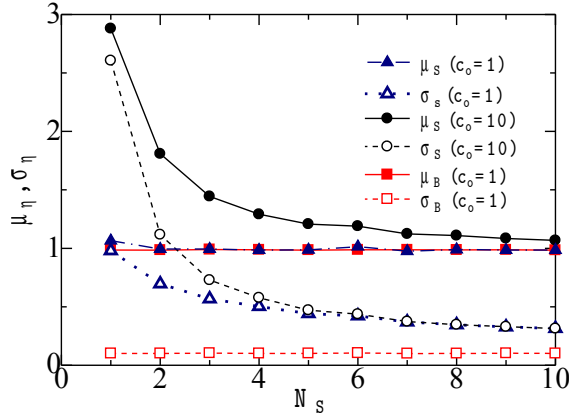


FIG. 14: (Color online) N_S dependences of μ_η and σ_η of system ($\eta = S$) and bath ($\eta = B$) with $N_B = 100$ and $T = 1.0$: filled (open) triangles denote μ_S (σ_S) with $c_o = 1.0$: filled (open) circles express μ_S (σ_S) with $c_o = 10.0$: filled (open) squares show μ_B (σ_B) with $c_o = 1.0$.

and 10, respectively, for which Eq. (32) yields $(a_S, b_S) = (1.18, 1.11)$, $(2.04, 2.05)$, $(4.50, 5.06)$ and $(9.82, 9.97)$. These values of a_S and b_S are not so different from N_S and $N_S\beta$ given by Eq. (29). We have employed the Γ distribution with these parameters a_S and b_S for our analysis of $f_S(u)$ having been shown in Fig. 13(a). Dashed curves in Figs. 15(a)-(d) express calculated Γ distributions, which are in fairly good agreement with $f_S(u)$ plotted by solid curves, except for $N_S = 1$ for which $g(0) = 0.0$ because $a_S = 1.18 > 1.0$ while $f_S(0) \neq 0.0$.

Similar analysis has been made for another result obtained with a larger $c_o = 10.0$ for

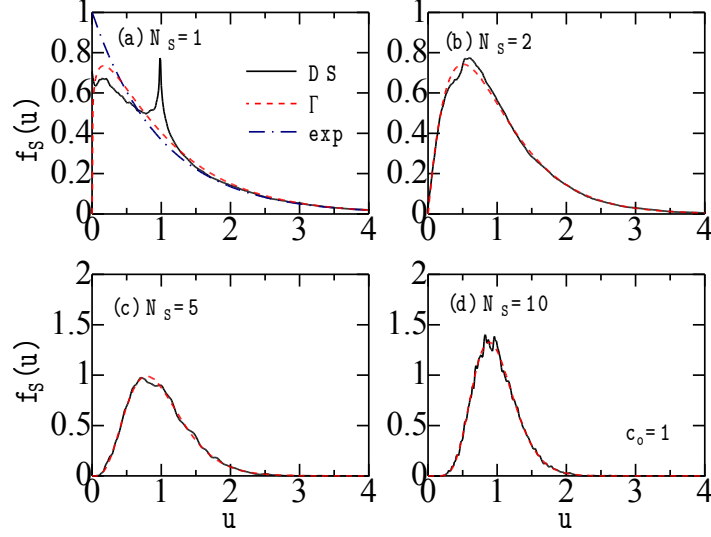


FIG. 15: (Color online) u dependences of $f_S(u)$ for (a) $N_S = 1$, (b) $N_S = 2$, (c) $N_S = 5$ and (d) $N_S = 10$ with $T = 1.0$, $c_o = 1.0$ and $N_B = 100$ obtained by DSs (solid curves): dashed and chain curves express Γ and exponential distributions, respectively (see text).

$N_B = 100$ and $T = 1.0$. N_S -dependences of calculated μ_S and σ_S are plotted by filled and open circles, respectively, in Fig. 14. Calculated (μ_S, σ_S) are $(2.88, 2.61)$, $(1.81, 1.12)$, $(1.21, 0.47)$ and $(1.07, 0.31)$ for $N_S = 1, 2, 5$ and 10 , respectively, which lead to $(a_S, b_S) =$

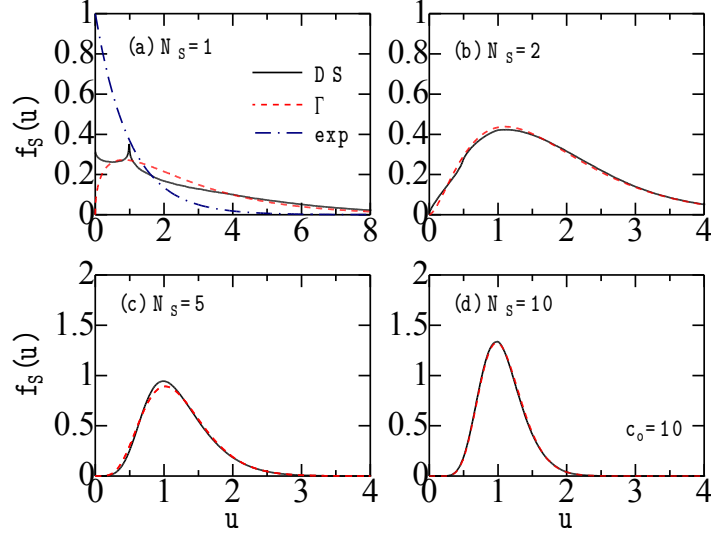


FIG. 16: (Color online) u dependences of $f_S(u)$ for (a) $N_S = 1$, (b) $N_S = 2$, (c) $N_S = 5$ and (d) $N_S = 10$ with $T = 1.0$, $c_o = 10.0$ and $N_B = 100$ obtained by DSs (solid curves): dashed and chain curves express Γ and exponential distributions, respectively (see text).

(1.22, 0.42), (2.62, 1.45), (6.57, 5.44) and (11.54, 10.81) by Eq. (32). Obtained a_S and b_S are rather different from N_S and $N_S\beta$ given by Eq. (29). Dashed curves in Figs. 16(a)-(d) show Γ distributions with these parameters, which may approximately explain $f_S(u)$ obtained by

DSs in the *phenomenologically* sense, except for $N_S = 1$ for which $g(0) = 0.0$ but $f_S(0) \neq 0.0$.

We note in Fig. 15(a) or 16(a) that an agreement between $g(u)$ and $f_S(u)$ with $N_S = 1$ is not satisfactory. We have tried to obtain a better fit between them, by using the q - Γ distribution $g_q(u)$ given by [10]

$$g_q(u) = \frac{1}{Z_q} u^{a-1} e_q^{-bu}, \quad (33)$$

with

$$e_q^x = [1 + (1 - q)x]_+^{1/(1-q)}, \quad (34)$$

where $[y]_+ = \max(y, 0)$ and Z_q is the normalization factor. Note that $g_q(u)$ reduces to the Γ distribution in the limit of $q \rightarrow 1.0$. Although the q - Γ distribution was useful for $f_S(u)$ of harmonic-oscillator systems subjected to finite bath [10], it does not work for $f_S(u)$ of double-well systems. This difference may be understood from a comparison between $f_S(u)$ for $N_S = 1$ of a double-well system shown in Fig. 15(a) [or 16(a)] and its counterpart of a harmonic oscillator system shown in Fig. 9(a) of Ref. [10]. Although the latter shows an exponential-like behavior with a monotonous decrease with increasing u , the former with a characteristic peak at $u = 1.0$ cannot be expressed by either the exponential, Γ , or q - Γ distribution.

B. Analysis of stationary position distributions

We have studied also the N_S dependence of stationary position distributions of $p(Q)$ and $P(\bar{Q})$, where Q denotes the position of a particle in the system and \bar{Q} expresses the averaged position given by

$$\bar{Q} = \frac{1}{N_S} \sum_{k=1}^{N_S} Q_k. \quad (35)$$

Figures 17(a) and 17(b) show $p(Q)$ and $P(\bar{Q})$, respectively, obtained by DSs for various N_S with $N_B = 100$, $T = 1.0$ and $c_o = 1.0$. For $N_S = 1$, we obtain $p(Q) = P(\bar{Q})$ with the characteristic double-peaked structure. We note, however, that $P(\bar{Q})$ is different from $p(Q)$ for $N_S > 1$ for which $P(\bar{Q})$ has a single-peaked structure despite the double-peaked $p(Q)$. This is easily understood as follows: For example, in the case of $N_S = 2$, two particles in

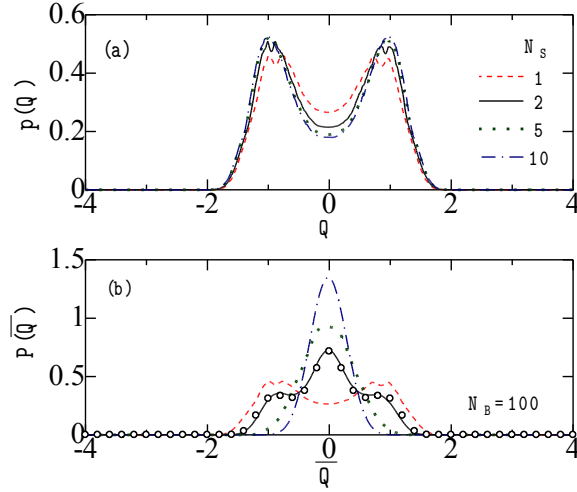


FIG. 17: (Color online) Stationary distributions of (a) $p(Q)$ as a function of particle position Q and (b) $P(\bar{Q})$ as a function of the averaged position \bar{Q} for various N_S : $N_S = 1$ (dashed curve), 2 (solid curve), 5 (dotted curve) and 10 (chain curve) with $N_B = 100$, $T = 1.0$ and $c_o = 1.0$. Open circles in (b) express an analytical result obtained by Eq. (36) with $N_S = 2$.

the system mainly locate at $Q_k = 1.0$ or $Q_k = -1.0$ ($k = 1, 2$) which yields the double-peaked distribution of $f_S(Q)$. However, the averaged position of $\bar{Q} = (Q_1 + Q_2)/2$ will be dominantly $\bar{Q} = 0.0$, which leads to a single-peaked $P(\bar{Q})$. The situation is the same also for $N_S > 2$.

Theoretically $P(\bar{Q})$ may be expressed by

$$P(\bar{Q}) = \int \cdots \int \prod_{k=1}^{N_S} dQ_k \exp[-\beta V(Q_k)] \delta\left(\bar{Q} - N_S^{-1} \sum_{k=1}^{N_S} Q_k\right). \quad (36)$$

$P(\bar{Q})$ numerically evaluated for $N_S = 2$ is plotted by open circles in Fig. 17 which are in good agreement with the solid curve expressing $P(\bar{Q})$ obtained by DS. It is impossible to numerically evaluate Eq. (36) for $N_S \geq 3$. In the limit of $N_S \rightarrow \infty$, $P(\bar{Q})$ reduces to the Gaussian distribution according to the central-limit theorem. This trend is realized already in the case of $N_S = 10$ in Fig. 17(b).

V. CONCLUDING REMARKS

We have studied the properties of classical double-well systems coupled to finite bath, employing the $(N_S + N_B)$ model [10] in which N_S -body system is coupled to N_B -body bath. Results obtained by DSs have shown the following:

- (i) Chaotic oscillations are induced in the double-well system coupled to finite bath in the absence of external forces for appropriate model parameters of c_o , N_B , T , $\{\omega_n\}$ and E_{So} ,
- (ii) Among model parameters, $f_S(u)$ depends mainly on N_S , c_o and T while $f_B(u)$ depends on N_B and T for $N_S \ll N_B$,
- (iii) $f_S(u)$ for $N_S > 1$ obtained by DSs may be phenomenological expressed by the Γ distribution,
- (iv) $f_S(u)$ for $N_S = 1$ with $c_o \neq 0.0$ cannot be described by either the exponential, Γ , or q - Γ distribution, although that with $c_o = 0.0$ follows the exponential distribution, and
- (v) The dissipation is not realized in the system energy for DSs at $t = 0 - 1000$ with $N_S = 1 - 100$ and $N_B = 10 - 1000$.

The item (i) is in consistent with chaos in a closed classical double-well system driven by external forces [23], although chaos is induced without external forces in our open classical double-well system. This is somewhat reminiscent of chaos induced by quantum noise in the absence of external force in closed quantum double-well systems [27]. Effects of induced chaos in the item (i) are not apparent in $f_S(u)$ because u ($= u_S$) is ensemble averaged over 10 000 runs (realizations) with exponentially distributed initial system energies. Items (ii) and (v) are the same as in the harmonic-oscillator system coupled to finite bath [10]. The item (v) suggests that for the energy dissipation of system, we might need to adopt a much larger

$N_B (\gg 1000)$ [26]. The item (iv) is in contrast to $f_S(u)$ for $N_S = 1$ in the open harmonic-oscillator system which may be approximately accounted for by the q - Γ distribution [10]. It would be necessary and interesting to make a quantum extension of our study which is left as our future subject.

Acknowledgments

This work is partly supported by a Grant-in-Aid for Scientific Research from Ministry of Education, Culture, Sports, Science and Technology of Japan.

-
- [1] A. O. Caldeira and A. J. Leggett, Phys. Rev. Lett. **46**, 211 (1981).
 - [2] A. O. Caldeira and A. J. Leggett, Ann. Phys. **149**, 374 (1983).
 - [3] V. B. Magalinskii, Sov. Phys. JETP **9**, 1381 (1959).
 - [4] P. Ullersma, Physica **32**, 27 (1966); *ibid.* **32**, 56 (1966); *ibid.* **32**, 74 (1966); *ibid.* **32**, 90 (1966).
 - [5] P. Hanggi, Gert-Ludwig Ingold and P. Talkner, New Journal of Physics **10**, 115008 (2008).
 - [6] Gert-Ludwig Ingold, P. Hanggi, and P. Talkner, Phys. Rev. E **79**, 061105 (2009).
 - [7] S. T. Smith and R. Onofrio, Eur. Phys. J. B **61**, 271 (2008).
 - [8] Q. Wei, S. T. Smith, and R. Onofrio, Phys. Rev. E **79**, 031128 (2009).
 - [9] J. Rosa and M. W. Beims, Phys. Rev. E **78**, 031126 (2008).
 - [10] H. Hasegawa, Phys. Rev. E **83**, 021104 (2011).
 - [11] A. Carcaterra, and A. Akay, Phys. Rev. E **84**, 011121 (2011).
 - [12] H. Hasegawa, J. Math. Phys. **52**, 123301 (2011).
 - [13] H. Hasegawa, Phys. Rev. E **84**, 011145 (2011).
 - [14] C. Jarzynski, Phys. Rev. Lett. **78**, 2690 (1997); Phys. Rev. E **56**, 5018 (1997).
 - [15] M. Thorwart, M. Grifoni, and P. Hänggi, Annals Phys. **293**, 14 (2001).
 - [16] H. Hasegawa, arXiv:1205.2058.
 - [17] L. Gamaitoni, P. Hänggi, P. Jung, and F. Marchesoni, Rev. Mod. Phys. **70**, 223 (1998).
 - [18] P. Hänggi, F. Marchesoni, and P. Grigolini, Z. Phys. B **56**, 333 (1984).
 - [19] P. Hänggi, , P. Jung, C. Zerbe, and F. Moss, 1993, J. Stat. Phys. **70**, 25 (1993).

- [20] L. Gammaitoni, E. Menichella-Saetta, S. Santucci, F. Marchesoni, and C. Presilla, Phys. Rev. A **40**, 2144 (1989).
- [21] A. Neiman and W. Sung, Phys. Lett. A **223**, 341 (1996).
- [22] H. Hasegawa, arXiv:1203.0770.
- [23] L. E. Reichl and W. M. Zheng, Phys. Rev. A **29**, 2186 (1984).
- [24] In the CL model ($N_S = 1$ and $N_B \rightarrow \infty$), we assume $c_n = a/\sqrt{N_B}$ (a : constant) because the kernel $\gamma(t)$ includes the c_n^2 term as given by $\gamma(t) = \sum_{n=1}^{N_B} c_n^2 (\cos \omega_n t / m \omega_n^2)$ which becomes $\gamma(t) = (2/\pi) \int J(\omega) (\cos \omega t / \omega) d\omega \propto \delta(t)$ in the limit of $N_B \rightarrow \infty$, $J(\omega)$ denoting the spectral density [see Eq. (20)].
- [25] A careless mistake was realized in $f_B(u)$ of Fig. 6(c) in Ref. [10], which should be nearly the same as that of Fig. 10(b) in this paper.
- [26] The recurrence time in a finite system is finite in the Poincaré recurrence theorem: H. Poincaré, Acta Math. **13**, 1 (1890), see also S. Chandrasekhar, Rev. Mod. Phys. **15**, 1 (1943).
- [27] A. K. Pattanayak and W. C. Schieve, Phys. Rev. Lett. **72**, 2855 (1994).